ELSEVIER

Symmetry of nonlinear optical response to time inversion of shaped femtosecond pulses as a clock of ultrafast dynamics

Tissa C. Gunaratne, Xin Zhu, Vadim V. Lozovoy, Marcos Dantus *

Department of Chemistry, Michigan State University, E. Lansing, MI 48824, United States

Abstract

Pulse shaping of femtosecond lasers causes frequency and intensity changes in the electromagnetic field; these changes can be symmetric or asymmetric with respect to time. Within the first few femtosecond, the nonlinear optical response is purely electronic. The nuclear response follows soon after that and continues for hundreds of femtoseconds. Differences in the nonlinear optical response caused by time inversion of laser pulses are explored here on a number of different systems. The change in behavior is first probed in a solution of IR144 for different laser intensities which shows a distinctive asymmetry upon time inversion in the fluorescence signal above the linear response regime. Two-photon induced fluorescence of a rhodamine B solution at high intensities is found to have a symmetric phase dependence which becomes asymmetric because of self phase modulation and self focusing at higher laser intensities. Surprisingly, the fragmentation and ionization of isolated *para*-nitrotoluene molecules was found not to depend on time inversion of the shaped laser pulses. However, from pulse shaping experiments we can glean the relative timing of the fragmentation processes. Results from this study show that the response of a system to time inversion of shaped femtosecond pluses provides an internal clock for ultrafast physicochemical processes occurring during laser–matter interactions.
© 2007 Elsevier B.V. All rights reserved.

Keywords: Pulse shaping; Coherent control; Two-photon microscopy; Quantum control

1. Introduction

Laser control of physicochemical processes is an area of research that continues to gain interest [1–3]. Progress has been fueled by technological advances in ultrashort pulse generation and the availability of pulse shapers capable of controlling the phase, amplitude and polarization state of hundreds of different frequencies within the bandwidth of the pulse. The number of different pulse shapes that can be accessed with the presently available technology is of astronomic proportions (10^{100}–10^{600}); therefore, it is impossible to experimentally evaluate the effect of every pulse shape. In this article we focus on the role of pulses having frequency–time characteristics that lack time-inver-

sion symmetry in laser control. Given that most processes are time dependent, one expects time asymmetric pulses to play an important role in laser control. The response of the system to a shaped pulse can be used as the first signature of the different physicochemical processes taking place, shedding light into their time scales. Reversing the time axis on the shaped pulse is the strategy used here to develop and later confirm our understanding of the processes occurring during strong field laser–matter interactions. With this strategy in mind we set out to test laser control of complex systems.

Conceptually, temporally asymmetric pulses can be considered a logical extension of the femtosecond pump-probe experiments of the 1980s [4,5] and the proposed pump-dump method for laser control of chemical reactions [6,7]. Clearly, in those cases the pump pulse initiates the molecular dynamics, and the probe (or dump) pulse monitors the progress of the dynamics as a function of time

* Corresponding author.
  E-mail address: dantus@msu.edu (M. Dantus).

delay between pump and probe. A shaped pulse can be considered to collectively contain both pump and probe pulses [8], and therefore reversing it in the time domain may cause a very different outcome if the pulse is asymmetric in the time domain. Note that not all shaped pulses are temporally asymmetric.

Evidence for the role of temporal asymmetry in laser pulses comes from some of the earliest experiments in femtosecond laser control by Shank and later by Wilson [9–11]. In these experiments, it was shown that fluorescence of laser dye molecules in solutions depended on the sign of the chirp of the laser pulse that induced it. This implied that the time ordering of the frequencies within the pulse had an important influence on the measured fluorescence yield and the ensuing dynamics. A number of theoretical explanations to these observations have been published. Experiments for which the shaped laser is one-photon resonant with the first excited state were the first ones to be fully understood [12–18].

The response of matter to ultrashort laser pulses can be generally explained by distinguishing three temporal regimes. The instantaneous response is purely electronic, taking place within the first 20 fs, is driven by the optical cycles, and at power densities above 10^{12} W/cm^2 involves ionization. The recoiling electron usually returns and scatters from the molecule, causing high-harmonic generation and further molecular fragmentation and ionization. Nuclear motion does not occur until 20–50 fs later, depending on the atomic mass. At low power densities ($<10^{12}$ W/cm^2), it is driven by the promotion of the system to excited states for which the initial ground state geometry is no longer a minimum energy configuration. For higher power densities, ionization leads to the accumulation of positive charges and strong repulsion, eventually resulting in a Coulomb explosion. The third temporal regime comes in to play after the first few hundred femtoseconds, involves the response of the bulk sample, and is relevant only to condensed phases. Given the time scales involved, coherence effects are expected only in the first two temporal regimes. Here we explore the effects of pulse shaping in liquid and gaseous states of matter, in order to study the electronic and initial nuclear response of the samples to shaped femtosecond pulses. Here we perform experiments on both the gaseous and the liquid phase with the same laser system and pulse shaping strategies. Our hope is to bridge the gap between separate measurements from different groups.

We start our study of the role of temporal symmetry in laser control with the excitation of laser dyes in solution. We then explore the effects of temporal symmetry on the fragmentation of isolated molecules. Research aimed at laser control of chemical reactions seeks to control molecular fragmentation with intense and shaped near-IR pulses [19,20]. These experiments involve complex energy landscapes and no simple explanations have been given as to why certain shaped pulses appear to optimize the production of some fragments over the others. Here, we look at a case for which pulse shaping causes order of magnitude changes in the fragmentation patterns [21].

Before delving into the complex systems discussed in this article, we briefly review cases that are better understood. When the response of the sample is linear with the laser field, such as in one-photon excitation, the integrated yield of the product is proportional to the integrated spectral density of the field, which does not depend on the spectral phase or time-inversion of the laser pulse. In agreement with the Brumer–Shapiro Emperor's New Clothes Theorem, time ordering of the field will have an effect only when two or more photons interact with the closed stationary system [22]. Experiments on control of chemical processes in the linear regime usually rely on spectral amplitude shaping, which serves to change the excitation intensity and perhaps the initial state populations [23,24]. Work on isolated diatomics demonstrated that chirp causes changes in the ensuing wave packet dynamics (spreading and revival times), but not on the excitation probability of the first excited state [25,26]. Note that the total population excited by the first pulse is independent of chirp. When using a second pulse to probe the wave packet dynamics, the overall experiment can no longer be consider linear in the laser field. We provide new evidence for the departure from the linear regime for a large organic molecule in solution.

Not all nonlinear optical processes depend on time inversion. Second harmonic generation in a thin frequency doubling crystal, for example, is an instantaneous response and its intensity is insensitive to time inversion. Here we remark that understanding the response of different nonlinear interactions to time inversion requires special consideration [27]. If the system undergoes very fast relaxation compared to the pulse duration, the system loses its sensitivity to time ordering due to decoherence, and then time inversion causes no effect. When relaxation times and the time scale of molecular dynamics are comparable to time-domain features of the field, one should expect a non-symmetric response to time inversion. Studying laser control with shaped laser pulses allows us to determine how the system responds to some of the simplest waveforms and determine the time scales and nature of the physicochemical processes occurring within the time scale of our femtosecond pulses. Results from gas, and liquid state samples are given to illustrate a wide range of behaviors. This article analyzes the symmetry of the nonlinear optical response of different systems to time inversion of the laser control field. These observations provide an internal clock for the ultrafast physicochemical processes occurring during intense laser–matter interactions.

2. Experimental

Experiments were carried out using a regeneratively amplified Ti:Al$_2$O$_3$ laser (Spitfire-Spectra Physics) seeded with a broad-band Ti:Al$_2$O$_3$ oscillator (KM Labs, 45 nm FWHM). Phase distortions, second and higher order, from the laser and any optics in the setup were eliminated using

multiphoton intrapulse interference phase scan (MIIPS) [28–30]. MIIPS uses a frequency-domain pulse shaper to introduce a well calibrated reference phase function to measure, at the location of the sample, spectral phase distortions in the laser pulses. This is a radically different approach compared to established methods, which use correlation between two or more pulses to retrieve the phase distortions by iterative simulation of the electric field. The phase dependence of nonlinear optical processes such as second-harmonic generation (SHG) is well understood [31,32] As the reference phase is scanned across the spectrum, a MIIPS trace is obtained and used to directly calculate the second derivative of the phase without the need for inversion algorithms. This phase is used to compensate the pulse to achieve bandwidth-limited pulses. The fully automated process is completed with unprecedented accuracy in a few seconds. A few research groups are beginning to use MIIPS since it became commercially available. With MIIPS, phase distortions are reduced below 0.01 rad within the FWHM and 0.1 rad across within the entire spectrum of the laser pulses; GVD measurements of quartz agree within 0.5 fs^2, and SHG spectra obtained with shaped pulses are in excellent agreement with theoretical calculations [29]. The same pulse shaper used for MIIPS was used to generate different spectral-phase functions for our experiments. The output laser pulses were centered at 800 nm with 750 μJ/pulse at 1 kHz. A small fraction of this output was spatially filtered with a 100 μm pinhole located within an up-collimating Keplerian telescope with 300 mm and 600 mm lenses.

In order to explore temporal symmetry brought about by pulse shaping, we chose four different spectral-phase functions, each depending on a single parameter. This allowed us to evaluate a complete range for each parameter with very good signal-to-noise statistics; the standard deviation was less than 10% for all our measurements. The different pulses generated are shown in Fig. 1. The phase functions $\phi(\omega)$ that we used are given by Eq. (1).

$$\phi = \alpha|\omega - \omega_0| + \pi \sin\{\gamma(\omega - \omega_0) - \delta\} + 1/2\beta(\omega - \omega_0)^2$$
(1)

where ω_0 is the carrier frequency and α, β, γ, and δ are variables used to introduce different phase functions independent of each other. We concentrate our attention on changes caused by time reversal of the waveform. Changing the sign of the phase function, while keeping the spectrum constant, provides time reversal [27]. The time–frequency behavior of the pulse can be characterized by its Wigner representation shown in Fig. 1 for the different shaped pulses. We note that the generation of these phase functions accurately using an acousto-optic programmable dispersive filter (AOPDF), a pulse shaper that is used by some groups, without affecting the spectrum of the laser pulses (changes in amplitude) is essentially impossible.

The first pulse shaping method used consists of splitting the pulse into two portions (high and low frequency) and introducing a time delay for each portion by changing

the slope of the phase in each frequency region (see Fig. 1a). The delay between the two pulses is 2α, in fs (Fig. 1a, where $\beta = \gamma = \delta = 0$).

The second pulse shaping method corresponds to linear chirp, which depends on the well-known chirp parameter β in fs^2 (Fig. 1b, where $\alpha = \gamma = \delta = 0$). In this case, the intensity profile for positively ($\beta > 0$) and negatively ($\beta < 0$) chirped pulses is identical. However, changes in the carrier frequency as a function of time have the opposite sign for positively and negatively chirped pulses. Notice the similarities between scanning α and scanning β.

The third and fourth parameters involve the use of a sinusoidal phase function, in which the period γ in fs (Fig. 1c where $\alpha = \beta = \delta = 0$) and phase δ of the periodic phase modulation (Fig. 1d, where $\alpha = \beta = 0$ and $\gamma = 35$ fs) were scanned. In each panel of Fig. 1, we show the spectral phase used, the intensity of the pulse as a function of time, and the calculated Wigner function of the pulse. In the case of sinusoidal modulation, with $|\delta| = \pi/2$, the intensity profile in time domain is almost symmetrical. The imperfections in Fig. 1d are due to the slightly asymmetric spectrum of the laser. Changing the sign of the phase provides time inversion, as can be confirmed by the Wigner presentation.

Departure from the linear regime was studied using a 10^{-4} M solution of IR144 in methanol and the resulting fluorescence was measured with a compact spectrometer in the 850–880 nm wavelength range. For these experiments we did not use a lens to focus the beam. The beam spot size (when intensity drops to $1/e^2$) is 8.3 mm. Three different energies per pulse were used, 0.7, 10, and 70 μJ/pulse. When the pulse is transform limited (TL) these energies give peak power densities, taking into account the maximum in the Gaussian beam distribution, of 1.8×10^7, 2.6×10^8, and 1.8×10^9 W/cm^2 peak power densities. The response of two-photon induced fluorescence was studied using a 10^{-4} M solution of rhodamine B in methanol and the resulting fluorescence was measured with a compact spectrometer in the 550–650 nm wavelength range. Experiments were carried out at 0.7, 10, and 15 μJ/pulse. The first two measurements using a (230 mm fl) curved mirror, achieving a 7.0 μm spot size. The highest intensity was reached using a 5× 0.1 numerical aperture microscope objective, which provides a spot size of 2.5 μm. Phase distortions introduced by the microscope objective were eliminated using MIIPS. The peak power densities for these measurements were calculated using $P = 2E/(\pi\tau w^2)$, where E is the energy per pulse, w is the spot size, and τ is the full-width at half maximum for TL pulses. For two-photon excitation the peak power density values used were 2.6×10^{13}, 3.7×10^{14}, and 4.4×10^{15} W/cm^2.

The interaction of shaped laser pulses on isolated gas phase polyatomic molecules was carried out with 150 μJ/pulse with the laser tightly focused by a 50 mm lens. The maximum power density reached 10^{16} W/cm^2 at the focus for TL pulses. The sample *para*-nitrotoluene (*p*-NT) was introduced through a leak valve in a chamber kept at
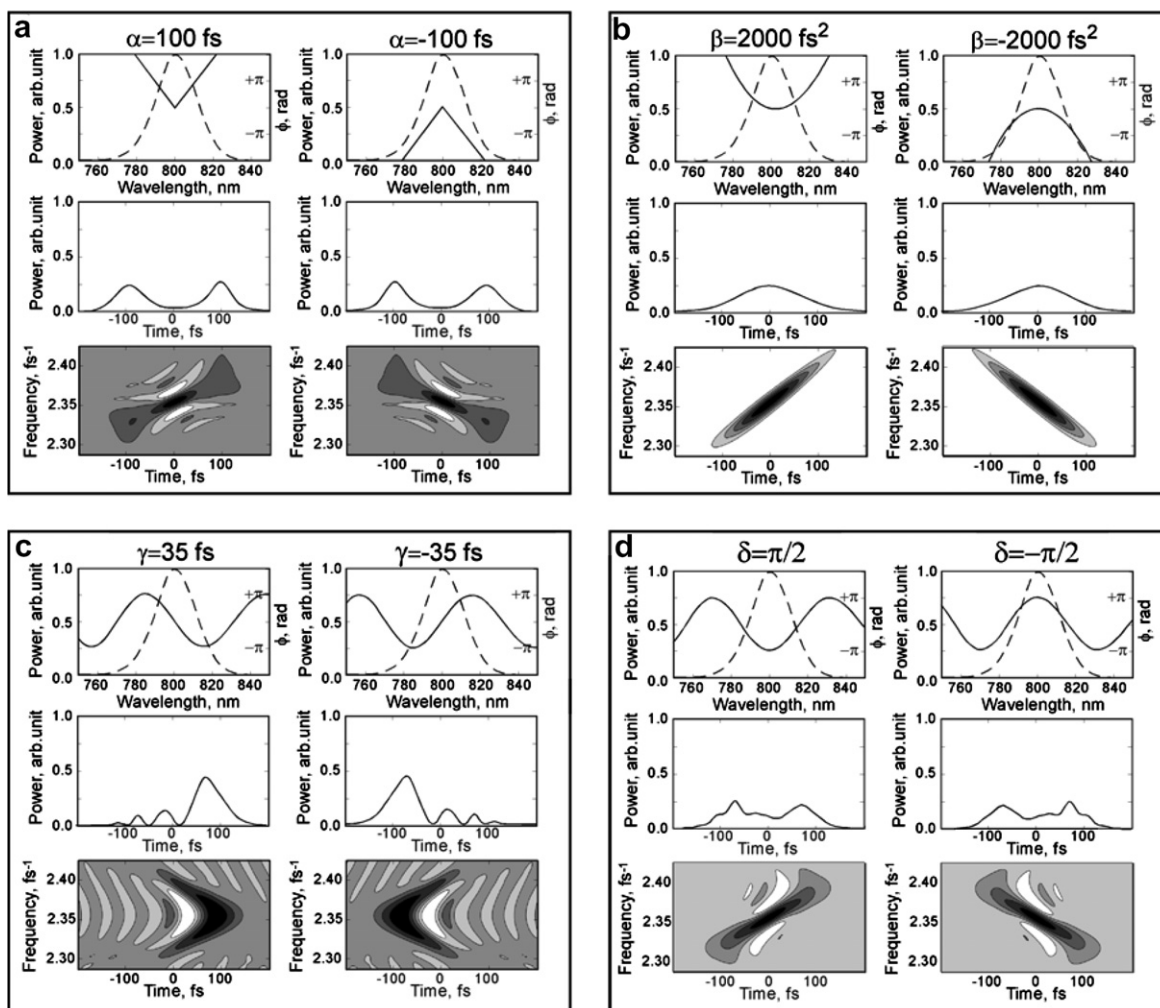
Fig. 1. Theoretical simulations showing temporal behavior of the pulses in the time domain and in the time–frequency domain (Wigner function) for the four different types of phase shaped pulses used in this study. (a) Pulse shaping by the parameter α results in splitting of the pulse into two portions. (b) Pulse shaping by scanning the parameter β controls the magnitude of chirp in the pulse. (c) Pulse shaping by scanning the parameter γ changes the periodicity of the sinusoidal function. (d) Pulse shaping by changing the phase of the parameter δ, changes the pulse in the time and frequency domain.

10^{-5} Torr under fast flow conditions to prevent the accumulation of photoproducts. The resulting fragment ions were detected by a time-of-flight mass spectrometer.

3. Results

The measured SHG spectrum, recorded using a 50 μm β-BBO crystal, as a function of the four different pulse shaping parameters is shown in Fig. 2. In Fig. 2a, it becomes clear that as the absolute value of the parameter α increases two distinct pulses are formed. In the SHG spectrum, we see intensity near 397 nm and 407 nm corresponding to the high and low frequency portions, respectively. There is a clear maximum when $\alpha = 0$, as expected. The data show a mild asymmetry (<10%). This minor effect is caused by a slight asymmetry in the laser spectrum and slight imperfections in the shaped laser pulse caused by phase wrapping to accommodate large phase retardations [33]. In Fig. 2b we see the effect of chirp. Notice that there is a small change in the spectrum, and

that the maximum SHG takes place for TL pulses, when $\beta = 0$. In Fig. 2c, we observe the effect from scanning γ. Notice that again the maximum is observed for $\gamma = 0$, and that significant intensity is observed out to $\gamma = \pm 50$ fs. For the first three cases in Fig. 2, the signal is symmetric with respect to sign inversion of the phase modulation in the frequency domain, or equivalently, inversion of field in time domain. This is because SHG is an instantaneous process that does not depend from the time ordering of the electric field and its interaction with the thin SHG crystal. Finally, in Fig. 2d, we observe the effect from scanning δ. Notice that the maximum in the SHG spectrum scans from long to short wavelengths creating straight parallel lines separated by π. The changes in the spectrum are caused by multiphoton intrapulse interference [31,32]. These features have been studied extensively because they are used to characterize femtosecond pulses by the MIIPS algorithm [28–30].

We first explored the excitation of IR144, which has a large cross section (10^{-16} cm^2) at 800 nm. For these exper-
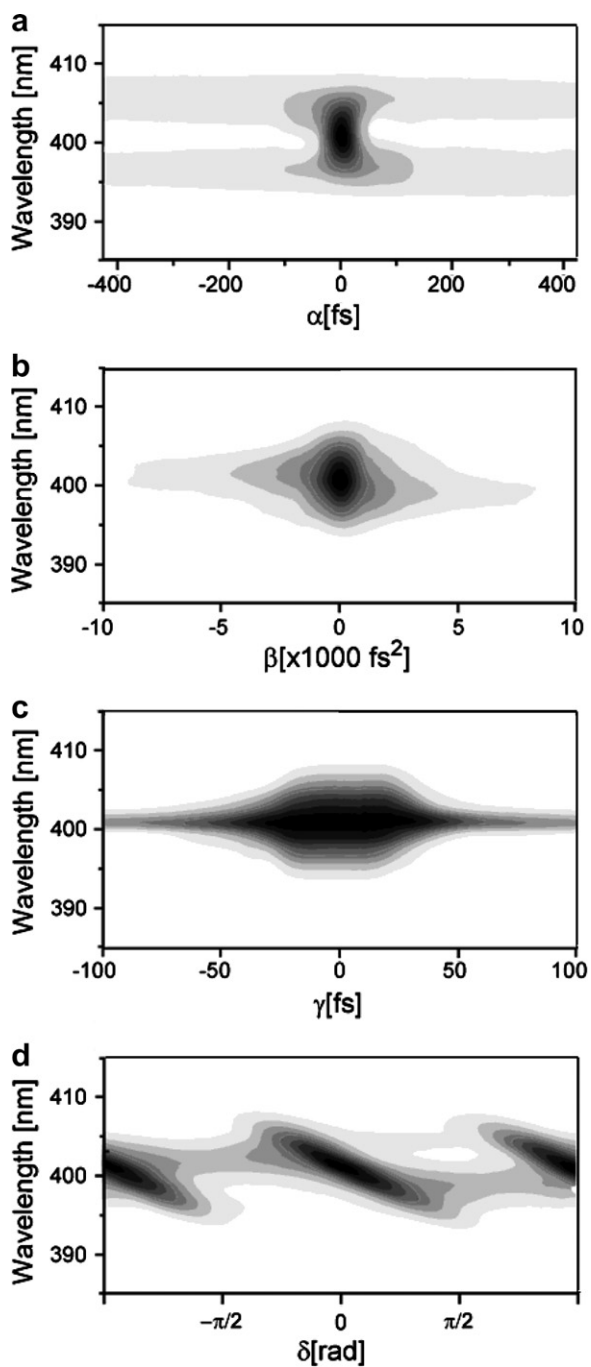
Fig. 2. Second harmonic generation spectrum recorded as a function of the four different phase functions; α, β, γ, and δ.

Fig. 3. Integrated fluorescence of IR144 recorded with different phase functions at two laser intensities 1.8×10^7 W/cm^2 (no phase effect) and 1.8×10^9 W/cm^2.

iments, we did not focus the laser and we attenuated until we reached a peak power density of 1.8×10^9 W/cm^2. These measurements, shown in Fig. 3, are consistent with the experiments by Shank et al. [9], and more recently discussed in depth by Gerber et al. [34]. Maximum fluorescent signal is observed for positive chirp. Upon excitation with a femtosecond pulse, IR144 exhibits a red shift associated with motion of the electronic state wave packet moving away from the Franck-Condon region. These dynamics have been observed in pump-probe experiments which
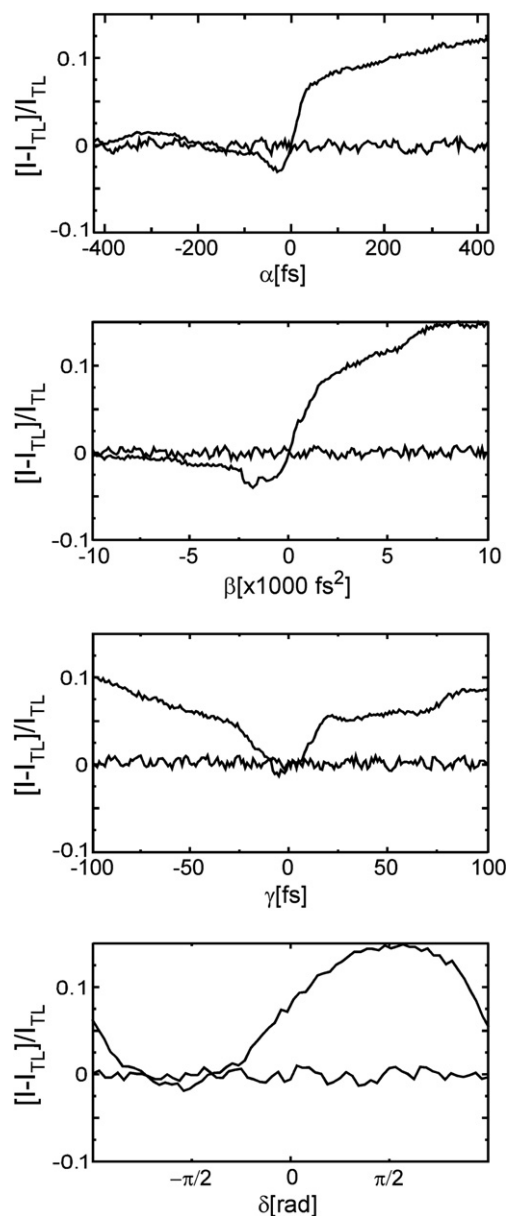
show a fast decay (200 fs) in the dynamic absorption at 808 nm, and a corresponding rise at 864 nm [35]. The correct interpretation of the data is that fluorescence is suppressed by stimulated emission, which is only possible when the wave packet is formed by the bluer frequency pump pulse and probed by the redder frequency pulse. Stimulated emission results in less fluorescence, and it is observed for TL pulses as well as for negative α, β, and δ. Therefore, positive chirp or a positive α delay of the bluer wavelengths prevents suppression and leads to greater fluorescence. As gamma is increased, stimulated emission becomes less efficient. In the delta scans, when $\delta = -\pi/2$ suppression is maximal and when $\delta = \pi/2$ suppression is minimal, a result that echoes the chirp results.

Notice that experiments carried out at 1.8×10^7 W/cm^2 no longer show the phase dependence. However, at 2.6×10^8 W/cm^2, that dependence was well above the noise (data not shown).

Results of pulse shaping on two-photon excitation of rhodamine B in solution are shown in Fig. 4. At low intensities optimum two-photon excitation is maximized for TL pulses as expected for a system undergoing a two-photon transition in the absence of an intermediate state and the results are symmetric. When we increased the intensity of the pulses so that the peak power density at the focus for TL pulses changes from 3×10^{13} to 4×10^{14} W/cm^2, continuum generation caused by self-phase modulation (SPM) was observed in the excitation beam after the fluorescence

cell, but the signal remained symmetric. These results are very different than those observed for one-photon excitation of laser dyes shown in Fig. 3, which were first explained by Shank et al. [9]. For intense one-photon excitation, positive chirp maximizes the fluorescence, while negative chirp favors stimulated emission, and results in a lower fluorescence yield. We found that for positive values of α, β, and γ near TL, there was a maximum in the SPM which caused a loss of up to 25% of the spectral intensity within the full width at half maximum of the pulse due to spectral broadening. Experiments carried out at 4×10^{15} W/cm^2 peak power density (see Fig. 4, thick lines) show changes in the fluorescence patterns, with higher signal for negative α and β values. Both the solvent and sample molecules are undergoing ionization at these intensities. The fluorescent signal shows less modulation depth, an indication of saturation, an observation that is particularly clear for the δ scan in Fig. 4d. Self-focusing and SPM (both third-order effects caused by the solvent) are much more pronounced at these intensities and are responsible for the observed changes.

The effect of time-reversal of the shaped pulses was explored for high intensity laser induced photofragmentation and ionization of isolated *p*-NT molecules as measured by time of flight mass spectrometry. For these experiments, the signal corresponds to the relative intensity of each frag-
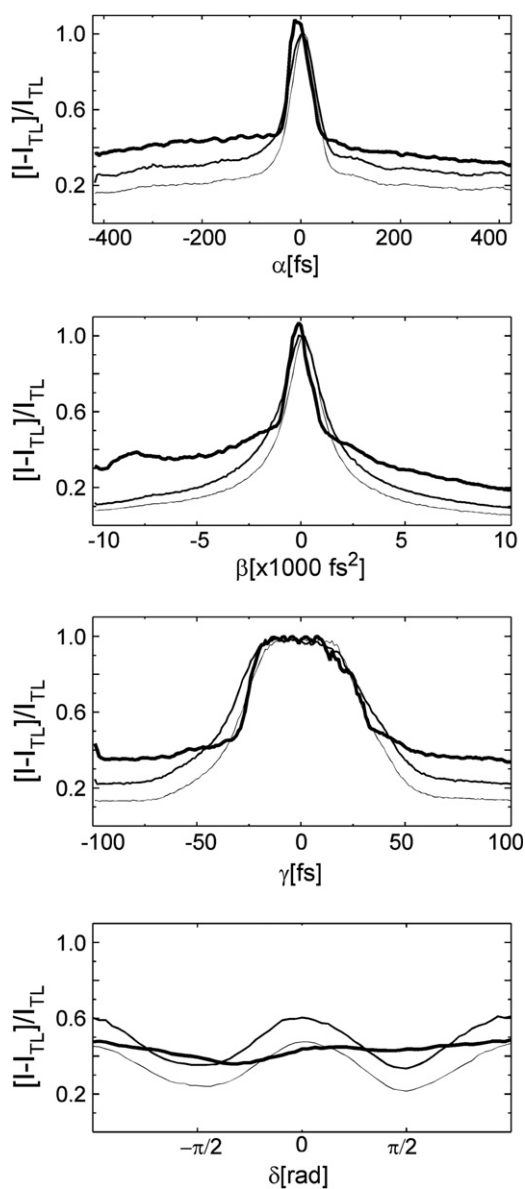

Fig. 4. Experimental changes in rhodamine B two-photon induced florescence recorded for different pulse shaping functions at 2.6×10^{13} W/cm^2, 3.7×10^{14} W/cm^2, and 4.4×10^{15} W/cm^2 (thin, medium and thick lines, respectively).
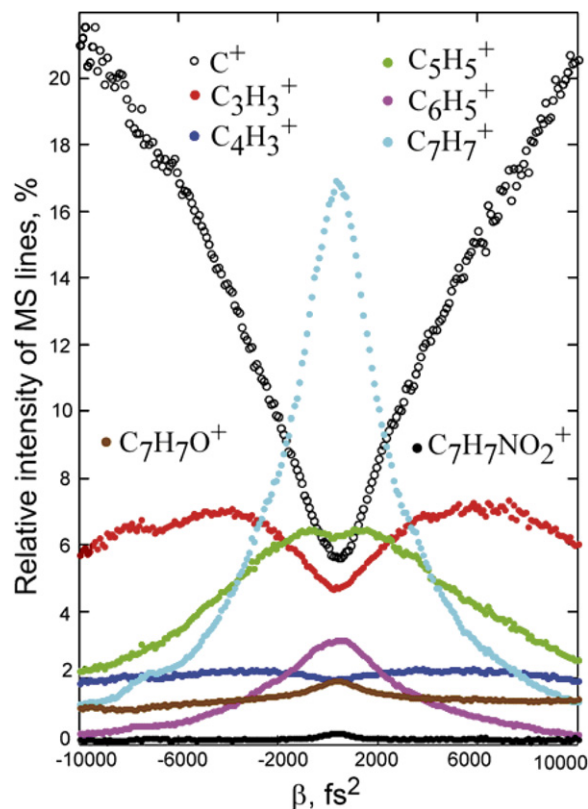

Fig. 5. Photo fragmentation and ionization of *p*-NT as a function of linear chirp were recorded by a time-of-flight mass spectrometer. The vertical axis is a measure of the fragment-ion yield relative to the total ion yield for each shaped pulse.

ment ion that is produced. Fig. 5 presents the changes in relative intensity as a function of chirp (β). The first interesting observation is that changes are essentially symmetric with respect to the sign of chirp. This implies that the different photofragmentation-ionization pathways have no dependence on the detailed frequency-time properties of the laser pulse. As we look further at the details we see that the smaller fragments C^+, $C_3H_3^+$, and $C_4H_3^+$ increase in relative intensity as chirp increases, while the larger fragments $C_5H_5^+$, $C_6H_5^+$, and $C_7H_7^+$ decrease in relative intensity. There is no evidence in these data that a particular time–frequency shaped pulse opens a photofragmentation-ionization pathway that deviates from the smooth progressions found. Data as a function of α, γ, and δ were also obtained, and in all cases symmetric dependence with respect to time ordering was observed.

4. Discussion

In this section, different nonlinear optical processes and their dependence on pulse shaping are examined. The general expectation is that the symmetry of the system response to time inversion of the pulse is a relatively simple concept that can be understood if we think about excitation with a shaped laser pulse from the point of view of a pump-probe experiment. Our results on IR144 are similar to those obtained by Shank and others, when the field is resonant with the fluorescent chromophore. However, we found that at 2.6×10^8 W/cm^2, the phase dependence was well above the noise, approximately 5% modulation. This implies that suppression of fluorescence due to stimulated emission takes place even at this relatively low intensity. These numbers are important when considering laser control experiments for which the laser is resonant with the sample, and exceeding them can lead to misleading results [23,24]. Nonlinear effects play an important role already at 10^8 W/cm^2, an intensity that is easy to reach with a femtosecond laser oscillator without amplification. For a discussion on the nonlinear effects that take place when molecules are subjected to femtosecond laser excitation, we recommend the review article by Pollard and Mathies [36]. Unfortunately, that review ignores the involvement of upper electronic states. Our measurements can be used as a rule of thumb. Nonlinear effects, which clearly show a dependence on the phase of the excitation pulses, take place when more than 0.3% of the molecules are being excited by the laser.

Experiments on two-photon excitation of rhodamine B, up to 9×10^{13} W/cm^2, were found to be fairly symmetric to time inversion. This implies that there is no analogy between the one-photon excitation experiments, for which stimulated emission plays such an important role, and two-photon excitation. Two-photon stimulated emission is much less probable than one-photon stimulated emission. Only at a peak power density of 1.0×10^{15} W/cm^2, we observe that negatively chirped pulses produce 10–20% more intense two-photon induced fluorescence. Our results for very strong peak power density show a similar phase dependence as found in the work of Zhang et al. in their closed-loop optimization of two-photon excitation of coumarin 515 under intense (10^{16} W/cm^2) excitation [37]. In their chirp dependence measurements, it is clear that negatively chirped pulses are approximately 15% more efficient for two-photon excitation than positively chirped pulses, however they ignore this effect and focus instead on an additional 5% enhancement observed for positive chirp $\sim$1000 fs^2. They invoked a two-photon excitation followed by a two-photon depletion model, similar to the model introduced by Shank for one-photon excitation of laser dyes under intense laser fields, to explain their findings. In our view, the two-photon stimulated excitation/depletion model is not consistent with the higher two-photon excitation observed for negative chirp values. The feature they observed at 1000 fs^2 may be caused by plasma formation by the extremely high field. At those intensities, filamentation occurs in the solvent and this process is accompanied by plasma formation [38–40]. This may explain the slight enhancement observed by Zhang et al. for positive chirp. We found evidence for SPM in the spectrum of the laser after the fluorescence cell. SPM was more significant in our case for TL pulses. We attribute SPM for the enhanced signal and not to molecular dynamics. We conclude that the observed asymmetric response at high peak power densities is purely dependent on nonlinear solvent effects. Under strong field excitation, negative chirp causes more efficient self focusing and self-phase modulation which cause an apparent enhancement of two-photon excitation.

Experiments on the interaction of high intensity near-IR pulses on isolated molecules, where we measured the relative yield of different fragment ions, show no evidence of asymmetry or response on time inversion. This result is unexpected if we think of different photofragmentation pathways that result from complex pump-probe experiments. One would consider that the fragmentation process could be influenced by the order in which sub-pulses arrive at the sample. However, our data are conclusive. No effect is observed. We also measured the dependence on α, γ, and δ. In all cases, all fragment ions behaved symmetrically with the pulse shaping parameters. Neither α or γ scans displayed evidence of a special period for which relative fragment ions are enhanced or suppressed. We speculate that the lack of asymmetry or resonance periods in the experiments on isolated molecules may be traced to the extensive power broadening taking place during a multiphoton ionization experiment. Bergman and coworkers have shown that multiphoton ionization is particularly sensitive to power broadening, as opposed to experiments that track fluorescence [41]. This is because probing takes place by the same pulse.

Given the high intensity of near-IR pulses used for these experiments (10^{16} W/cm^2, at TL), multiphoton ionization, occurring at energies well above the threshold of molecular ion formation, takes place within the duration of the pulse.

As the pulses begin to broaden due to phase shaping, we observe the generation of smaller fragments. Our explanation to this effect is that the longer pulses allow the atoms time to start to move away from their ground state equilibrium positions while the field is still on. The data allow us to assign a time scale for the different processes occurring during p-NT fragmentation. For p-NT, the first step is field ionization of the parent molecules occurring within the rise-time of the pulse. Next is NO and NO_2 loss. The next step involves the first, second, and third losses of C_2H_2 fragments occurring approximately after 0.1, 0.4, and 1 ps ending with C^+ which is still growing after $10\,000\,fs^2$ chirp. We recently finished a complete study on the photofragmentation of p-NT, that will be published elsewhere [42]. Preliminary results on benzene and acetophenone (data not shown) are symmetric for all the shape parameters, strengthening our argument for the response of isolated molecules being dominated by electronic effects.

5. Conclusions

The field of laser control has progressed at a very fast pace in the last decade. There are a number of cases that are well-established and understood. However, as the laser intensity increases, or the system becomes more complex, our understanding begins to falter. In this study we have taken one of the simplest parameters to understand, namely the arrow of time. We have explored the temporal evolution of shaped pulses using four different pulse shaping strategies that lead to generation of pulses that have different types of temporal symmetry or none at all. This allows us to think of time-dependent models similar to those of a pump-probe experiment, and put them to the test by reversing the field. We began our experiments with SHG, one- and two-photon excitation of organic dyes in solution, some of the better understood systems. We then turned our attention to more complex systems.

The response to time-inversion of shaped femtosecond pulses was found to be symmetric in all cases for which the signal depends on the electronic response or ionization of the system. Processes which take place on a faster time scale (0–20 fs) than the laser pulses, result in symmetric time responses as well. Clear asymmetry was found when the response of the system had a molecular dynamics component taking place in the 20–200 fs time scale, such as in the excitation of IR144 in solution.

Our experiments on IR144 help to establish the departure from the linear regime for highly conjugated organic molecules. We found that when the laser excites 0.3% of the sample molecules nonlinear processes begin to play a role and show up as phase dependence. The symmetry observed for two-photon fluorescence of rhodamine B indicates that molecular dynamics play a minor role. Any effects observed for two-photon induced fluorescent molecules in liquids can be assigned to SPM in the solvent, a conclusion we reach based on our experiments carried out at the highest peak power densities.

We were surprised to find that the strong-field excitation of isolated p-NT showed a symmetric response to time inversion. Our present understanding of this system combines two components. The first is very fast ionization, within the rising edge of the pulse, an electronic response that is expected to be symmetric to time inversion. The second, is excitation of internal molecular degrees of freedom. The observed temporal symmetry suggests that intramolecular dynamics and relaxation rates are faster than the duration of our laser pulses ($\sim$35 fs). Our data yield sufficient information to provide a time scale for the photodissociation processes occurring in the presence of the field. In conclusion, the nonlinear response symmetry to time inversion of shaped laser pluses can be used to provide a clock for the underlying ultrafast processes taking place during strong laser-matter interactions.

Acknowledgements

References

[1] V.V. Lozovoy, M. Dantus, Annual Reports on the Progress of Chemistry, Section C: Physical Chemistry 102 (2006) 227.
[2] V.V. Lozovoy, M. Dantus, ChemPhysChem 6 (2005) 1970.
[3] D. Goswami, Physics Reports – Review Section of Physics Letters 374 (2003) 385.
[4] T.S. Rose, M.J. Rosker, A.H. Zewail, Journal of Chemical Physics 88 (1988) 6672.
[5] M. Dantus, M.J. Rosker, A.H. Zewail, Journal of Chemical Physics 87 (1987) 2395.
[6] S.A. Rice, D.J. Tannor, R. Kosloff, Journal of the Chemical Society – Faraday Transactions 82 (1986) 2423.
[7] D.J. Tannor, R. Kosloff, S.A. Rice, Journal of Chemical Physics 85 (1986) 5805.
[8] C. Daniel, J. Full, L. Gonzalez, C. Lupulescu, J. Manz, A. Merli, S. Vajda, L. Woste, Science 299 (2003) 536.
[9] G. Cerullo, C.J. Bardeen, Q. Wang, C.V. Shank, Chemical Physics Letters 262 (1996) 362.
[10] C.J. Bardeen, V.V. Yakovlev, J.A. Squier, K.R. Wilson, S.D. Carpenter, P.M. Weber, Journal of Biomedical Optics 4 (1999) 362.
[11] A.H. Buist, M. Muller, R.I. Ghauharali, G.J. Brakenhoff, J.A. Squier, C.J. Bardeen, V.V. Yakovlev, K.R. Wilson, Optics Letters 24 (1999) 244.
[12] J. Cao, Journal of Luminescence 87–89 (2000) 30.
[13] J. Cao, C.J. Bardeen, K.R. Wilson, Physical Review Letters 80 (1998) 1406.
[14] J. Cao, C.J. Bardeen, K.R. Wilson, Journal of Chemical Physics 113 (2000) 1898.
[15] J. Cao, K.R. Wilson, Journal of Chemical Physics 106 (1997) 5062.
[16] J. Cao, K.R. Wilson, Physical Review A: Atomic, Molecular, and Optical Physics 55 (1997) 4477.
[17] J. Cao, K.R. Wilson, Journal of Chemical Physics 107 (1997) 1441.

[18] C.J. Bardeen, J. Cao, F.L.H. Brown, K.R. Wilson, Chemical Physics Letters 302 (1999) 405.
[19] A. Assion, T. Baumert, M. Bergt, T. Brixner, B. Kiefer, V. Seyfried, M. Strehle, G. Gerber, Science 282 (1998) 919.
[20] T. Brixner, G. Gerber, ChemPhysChem 4 (2003) 418.
[21] V.V. Lozovoy, T.C. Gunaratne, J.C. Shane, M. Dantus, Chem. Phys. Chem. 7 (2006) 2471.
[22] P. Brumer, M. Shapiro, Chemical Physics 139 (1989) 221.
[23] V.I. Prokhorenko, A.M. Nagy, R.J.D. Miller, Journal of Chemical Physics 122 (2005) 184502.
[24] V.I. Prokhorenko, A.M. Nagy, S.A. Waschuk, L.S. Brown, R.R. Birge, R.J.D. Miller, Science 313 (2006) 1257.
[25] V.V. Lozovoy, O.M. Sarkisov, A.S. Vetchinkin, S.Y. Umanskii, Chemical Physics 243 (1999) 97.
[26] V.V. Lozovoy, S.A. Antipin, F.E. Gostev, A.A. Titov, D.G. Tovbin, O.M. Sarkisov, A.S. Vetchinkin, S.Y. Umanskii, Chemical Physics Letters 284 (1998) 221.
[27] A.M. Weiner, Optics Letters 25 (2000) 1207.
[28] V.V. Lozovoy, I. Pastirk, M. Dantus, Optics Letters 29 (2004) 775.
[29] B. Xu, J.M. Gunn, J.M. Dela Cruz, V.V. Lozovoy, M. Dantus, Journal of the Optical Society of America B: Optical Physics 23 (2006) 750.
[30] I. Pastirk, B. Resan, A. Fry, J. MacKay, M. Dantus, Optics Express 14 (2006) 9537.
[31] K.A. Walowicz, I. Pastirk, V.V. Lozovoy, M. Dantus, Journal of Physical Chemistry A 106 (2002) 9369.
[32] V.V. Lozovoy, I. Pastirk, K.A. Walowicz, M. Dantus, Journal of Chemical Physics 118 (2003) 3187.
[33] M. Dantus, V.V. Lozovoy, Chemical Reviews 104 (2004) 1813.
[34] G. Vogt, P. Nuernberger, R. Selle, F. Dimler, T. Brixner, G. Gerber, Physics Review A 74 (2006).
[35] E.A. Carson, W.M. Diffey, K.R. Shelly, S. Lampa-Pastirk, K.L. Dillman, J.M. Schleicher, W.F. Beck, Journal of Physical Chemistry A 108 (2004) 1489.
[36] W.T. Pollard, R.A. Mathies, Annual Review of Physical Chemistry 43 (1992) 497.
[37] S. Zhang, Z.R. Sun, X.Y. Zhang, Y. Xu, Z.G. Wang, Z.Z. Xu, R.X. Li, Chemical Physics Letters 416 (2005) 346.
[38] W. Liu, O. Kosareva, I.S. Golubtsov, A. Iwasaki, A. Becker, V.P. Kandidov, S.L. Chin, Applied Physics B-Lasers and Optics 76 (2003) 215.
[39] A. Brodeur, F.A. Ilkov, S.L. Chin, Optics Communications 129 (1996) 193.
[40] W. Liu, S. Petit, A. Becker, N. Akozbek, C.M. Bowden, S.L. Chin, Optics Communications 202 (2002) 189.
[41] N.V. Vitanov, B.W. Shore, L. Yatsenko, K. Bohmer, T. Halfmann, T. Rickes, K. Bergmann, Optics Communications 199 (2001) 117.
[42] V.V. Lozovoy, X. Zhu, T.C. Gunaratne, D.A. Harris, J.C. Shane, M. Dantus, Journal of Physical Chemistry A, submitted for publication.